Turbulent Flow Characteristics Controlled by Polymers

Ruri Hidema, Naoya Yamada, Hiroshi Suzuki, and Hidemitsu Furukawa

Abstract An experimental study has been performed in order to investigate the relationship between the extensional viscosity of polymer solution and the turbulent drag reduction. A flexible polymer and a rigid rod-like polymer were added to the two-dimensional turbulent flow that was visualized by the interference pattern of a flowing soap film and analyzed by a single-image analysis. The power spectra of interference images were obtained, which is related to the water layer fluctuations in turbulence. The power spectra show a scaling behavior and the power components give the information of drag reduction. It was suggested that the energy transfer mechanisms are different in streamwise and normal directions. In the normal direction, the energy transfer was prohibited by the orientation of polymers, while the energy transfer in the streamwise direction was prohibited by extensional viscosity of polymers. The extensional viscosities of polymer solutions were measured by calculating pressure losses at an abrupt contraction flow.

1 Introduction

The addition of very small amounts of flexible polymer to a water flow reduces drag in a turbulent flow, which is known well as drag reduction phenomena, and used in many industries to improve the energy efficiency. Although this effect has been known for more than half a century, the physical mechanism that causes this drag reduction has been still unclarified. The first important work on the drag reduction was made by Lumley [1]. He argued the increase of the apparent viscosity in the

R. Hidema (✉) · H. Suzuki
Kobe University, Kobe, Hyogo, 657-8501, Japan
e-mail: hidema@port.kobe-u.ac.jp

N. Yamada · H. Furukawa
Yamagata University, Yonezawa, Yamagata 992-8510, Japan

Alexander K. Belyaev et al. (eds.), *Mechanics and Model-Based Control of Advanced Engineering Systems*, DOI 10.1007/978-3-7091-1571-8_18,

flow outside of the viscous sublayer is the key for drag reduction, which is due to the molecular extension of polymers. The extension of polymers occurs only under the rapid strain rates, and gives the anisotropic effects in the fluids. On the other hand, Tabor and de Gennes [2] suggested that the major effect arises only when the elastic energy stored by the partially stretched polymers becomes comparable to the turbulent energy.

However, both analyses have the shortcomings to explain which a strain works for stretching polymers, that is, shear strain or extensional strain. Smith et al. showed that DNA molecules were effectively stretched by extensional flow [3]. Indeed, extensional viscosity of polymers due to extensional strain can reach much higher compared to the intrinsic viscosity that is related to the shear viscosity. Thus, Hidema et al. [4] mentioned that an abrupt increase of the extensional viscosity depending on the extensional strain rate is the key for the turbulent drag reduction. In addition, the extensional viscosity is defined as a viscosity increase in an extensional axis, thus, the increase of the extensional viscosity is due to a flexibility of polymers, which leads anisotropic effects in the flow. In our previous study, we mentioned that a flexible polymer leads abrupt increase of extensional viscosity due to an abrupt extension of polymers in the flow and a rod-like rigid polymer leads slightly increase of the viscosity due to an orientation in extension axis [4, 5].

In this study, we focus on anisotropic effects of polymers on turbulent flow. A flexible polymer and a rod-like rigid polymer were chose to observe how the extensional viscosity works on turbulence drag reduction. In addition, the extensional viscosities of the polymer solution were measured by abrupt contraction flow to confirm our ideas.

In order to observe the turbulent flow affected by stretched polymers, two-dimensional turbulence made by flowing soap films is used (Fig. 1) [6]. As shown in Fig. 1c, both sides of the flowing soap films are free surfaces and the water layer is sandwiched by surfactants. The thickness of water layer is much larger than vanishingly small surfactant molecules, and also the surface area is infinity compared to the thickness. Additionally, surface tension is negligible due to the surfactant in the surface of flowing soap films. Therefore, soap film is considered as a 2D water layer flow. Soap films reflect illumination light, which make interference patterns of the film. Since interferences of the illumination lights are affected by the thickness of the water layer, the interference patterns have information of the dynamics of the water layer as 2D flows. When a grid is inserted to the flow, an extensional strain occurs at the grid, which causes polymer stretching or polymer orientation. Thus, in the case when polymers are added to the flow, the 2D grid turbulence is affected by the polymers. Flows are visualized and analyzed by a single-image processing, which is proposed by our previous work [8]. The extensional strain applied at this apparatus is roughly calculated by Eq. (1).

$$S(t) = S_0 \exp(-\dot{\varepsilon} t). \tag{1}$$

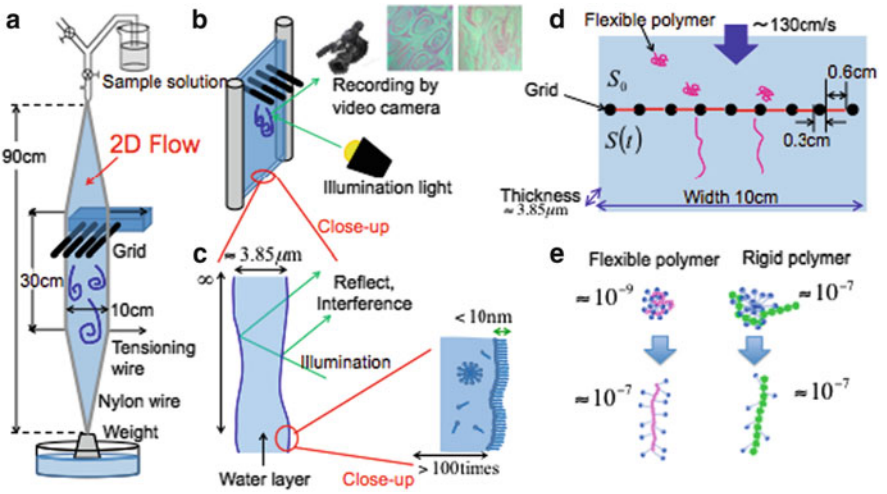

Fig. 1 The experimental set up of flowing soap films. (**a**) Is the whole image, (**b**) is the close up figure of the flowing soap film channel, (**c**) shows the cross section, (**d**) explains how the extensional strain occurs in this flow around the grid, (**e**) shows the expected polymer behavior under extensional strain measured by a dynamic light scattering technique [4]

where S_0 [m^2] is the cross-section area before deformation, $S(t)$ [m^2] is the cross-section area after deformation, t [s] is the time required for deformation and $\dot{\varepsilon}$ [s^{-1}] is the extensional rate. In our case, $\dot{\varepsilon}$ is calculated as 351 s^{-1} by the mean velocity, width of the flow, diameter of the grids and thickness of the film.

An extensional viscosity measured by an abrupt contraction flow is firstly proposed in this paper thus, the technique is described in the experimental section.

2 Experimental

2.1 Materials

For the 2D flow visualization experiments, soap solutions contained sodium dodecylbenzenesulfonate (SDBS) as a surfactant at the concentration of 2 wt%. As the flexible polymers, polyethyleneoxide (PEO, molecular weight of 3.5×10^6) was used at the concentration of 0.25, 0.5, 0.75, 1.0, 1.5 and 2.0×10^{-3} wt%. As the rod-like rigid polymers, hydroxypropyl cellulose (HPC, molecular weight is greater than 1×10^6) was used at the concentration of 0.01, 0.02 and 0.05 wt%. The overlap concentration of PEO was about 0.012 wt% and that of HPC was roughly 0.15 wt%. For the abrupt contraction flow experiments, the solution contains PEO or HPC at the same concentration of 2.0 wt%.

2.2 Turbulence Visualization by Flowing Soap Films

The experiments were carried out in an apparatus shown in Fig. 1. The thickness of water layer $h(t)$ [m] was about 3.85 μm with the mean velocity $V(t)$ [m/s] of 130 cm/s when the flow flux $Q(t)$ [m^3/s] was 0.5 ml/s, since there is the relationship like $h(t) = Q(t)/V(t)W$ where W [m] is the width of the soap film channel [6]. The interference images of soap films were recorded with a digital video camera (Panasonic TM700) at the data acquisition area, which was located at 20 cm behind the grid. The shutter speed of the video camera was 1/3,000 s. A time interval in a series of images was adjusted to 1/60 s. Each of the frames acquired by the camera was converted into RGB form files with a spatial resolution of 640 × 360 pixels.

2.3 Single-Image Processing by Film Interference Flow Imaging

The interference images were analyzed by a 2D-FFT, which calculated the power spectrum of the interference images [7]. Since the RGB pixel intensity of the images is related to the thickness of water layer, the power spectrum of the image shows the dynamics of 2D flows. Here, the power spectrum $\langle I^2(k_x, k_y)\rangle$ was calculated by the pixel intensity G with a hamming window, where the k_x [m^{-1}] and k_y [m^{-1}] are the spatial frequency that are streamwise and normal directions in an interference image. For measurements presented here, the data acquisition area that was clipped from the video frames has 256 × 256 pixels, which correspond to 2.56 × 2.56 cm^2, thus, the k_x and k_y range from 1/2.56 to 1/0.02 cm^{-1}, that is, 0.391–5.00 cm^{-1} as the frequency. $\langle I^2(k_x, k_y)\rangle$ of the pixel intensity G characterizes the strength of the thickness fluctuation of water layer on spatial frequency, k_x and k_y. Here the power spectrum in both frequencies are plotted to discuss energy transfer of turbulence in streamwise and normal directions.

2.4 Extensional Viscosity Measurements by Abrupt Contraction Flow

An abrupt contraction flow was made by connecting a syringe and a glass tube (Fig. 4a). The syringe that has a diameter, D_1 [m], of 28 mm was filled with a polymer solution. The polymer solution was forced out of the syringe into the glass tube that has a diameter of 2.3 mm, D_2 [m]. The forces F [N] to push the solution at the flow rates of 5, 10, 20 and 30 ml/min were measured by a load cell. A pressure P_{EX} [Pa] added to the flow was calculated by F [N], as $P_{EX} = F/A_1$ when A_1 [m^2] is a cross area of the syringe. First, the experimental pressure P_{EX} [Pa] was calculated by water to calculate the friction of the syringe, P_F [Pa].

An energy-balance equation is written as

$$P_{\mathrm{EX}} + P_0 + \frac{1}{2}\rho V_1^2 = \Delta P_1 + \Delta P_2 + \Delta P_3 + \Delta P_4 + P_0 + \frac{1}{2}\rho V_2^2 + P_F + P, \quad (2)$$

where P [Pa] is an extensional stress, P_0 [Pa] is the atmosphere pressure, V_1 [m/s] and V_2 [m/s] are velocities in the syringe and the glass tube, ρ [kg/m^3] is the density, and ΔP_1 [Pa], ΔP_2 [Pa], ΔP_3 [Pa] and ΔP_4 [Pa] are the pressure drop in the syringe, in the glass tube, at the abrupt contraction in the middle of the flow and at the abrupt expansion in the end of the glass tube, which is calculated as follows:

$$\begin{aligned} &\Delta P_1 = \frac{64\mu}{V_1 D_1}\frac{l}{D_1}\frac{V_1^2}{2}, \Delta P_2 = \frac{64\mu}{V_2 D_2}\frac{l}{D_2}\frac{V_2^2}{2}, \Delta P_4 = \frac{V_2^2}{2}\rho, \\ &\Delta P_3 = \zeta\frac{V_2^2}{2}\rho, \zeta = 0.04 + \left(1 - \frac{D_2}{D_{\mathrm{C}}}\right)^2, \frac{D_{\mathrm{C}}}{D_2} = 0.582 + \frac{0.0418}{1.1 - \sqrt{D_2 - D_1}} \end{aligned} \quad (3)$$

P_F is calculated by measuring P_{EX} of water. Additionally, only the ΔP_2 should be considered to calculate extensional viscosity since ΔP_1, ΔP_3 and ΔP_4 are much less than P_F. Thus, the extensional viscosity η_e [Pa s] was calculated as follows. Here, extension rate $\dot{\varepsilon}$ is calculated by considering a previous research [8].

$$P = P_{\mathrm{EX}} - P_F - \Delta P_2 = \eta_e \dot{\varepsilon}, \dot{\varepsilon} = \frac{0.75 V_2}{D_2/2} \quad (4)$$

By measuring the P_{EX} of polymer solution, the extensional viscosities of polymers were calculated.

3 Results and Discussion

Figure 2 shows the examples of interference patterns of 2D grid turbulence. Turbulence was generated at the comb, and was convected in the observation area. The interference patterns of 2D turbulence visualize the thickness of water layer fluctuations, which is considered as a passive scalar. One of the characteristics of 2D turbulence is an inverse energy cascade from small scales to large scales that is seen through the increase of the apparent size of the eddies compared to injection scales. By adding of polymers, the eddies clearly become long in streamwise direction and narrow in normal direction (Fig. 2b, c). This feature is especially seen in the case of the addition of PEO. This indicates that the polymer inhibits inverse energy transfers in normal direction. In the case of the addition of HPC, the effect can be slightly observed at much higher concentration compared with that in the case of PEO.

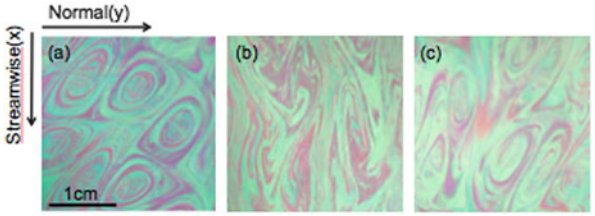

Fig. 2 Interference images of the turbulence in flowing soap films. The images are taken at SDBS 2 wt% solution (**a**), + PEO 2.0×10^{-3} wt% solution (**b**), + PEO HPC 0.05 wt% (**c**) for a mean velocity is about 130 cm/s. The *black bars* indicate 1 cm

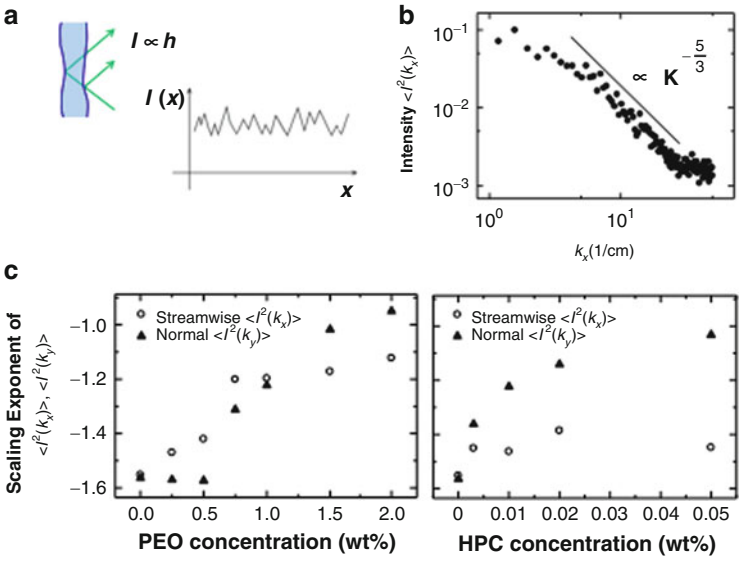

Fig. 3 The example of the power spectra $\left\langle I^2(k_x, k_y)\right\rangle$. The k_x and the k_y directions in the image represent the spatial frequencies in the streamwise and the normal directions

Figure 3 shows the example of the power spectra $\left\langle I^2(k_x, k_y)\right\rangle$ of the interference pattern. As shown in Fig. 3a, the pixel intensity is related to the thickness. k_x [m^{-1}] and k_y [m^{-1}] in $\left\langle I^2(k_x, k_y)\right\rangle$ are the spatial frequencies which have the information of water layer fluctuations directed in streamwise and normal directions. $\left\langle I^2(k_x, k_y)\right\rangle$ shows the examples of the scaling behaviors (Fig. 3b). It is found that the power component almost fits with the $-5/3$ that is theoretically predicted for a 2D turbulence. The variation of the power components is shown in Fig. 3c. In the case of PEO is added, the value was changed from $-5/3$ to -1 in both streamwise and normal directions. At lower concentrations of PEO, the variation rate of the power component is small but the rate increases rapidly from 0.5 to 0.75×10^{-3} wt%. In the case of HPC is added, the value was changed gradually from $-5/3$

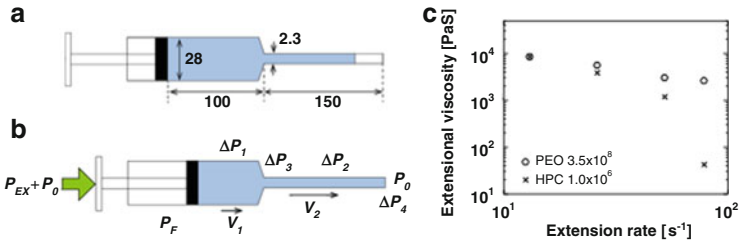

Fig. 4 An abrupt contraction flow and calculated extensional viscosities

to −1 in normal directions. However, the variation of the scaling exponent in the streamwise direction was small and has the absence of a pattern in the case of HPC. As mentioned above, in 2D turbulence, an inverse energy cascade is a characteristic phenomenon. The inverse energy cascade is seen through the vortex mergers in the interference patterns. The scaling exponent detects the prohibition of the inverse energy cascade due to polymers, that is, the variation from −5/3 to −1. Thus, it is considered that PEO prohibit the inverse energy cascade in both directions, while HPC prohibits the inverse energy cascade only in the normal direction. This difference is due to the different mechanism of energy transfer in turbulence when polymers are added. In the normal direction, the orientation of polymers prohibits the energy transfer. Thus it is happen in both PEO and HPC cases. On the other hand, the extensional viscosity prohibits the energy transfer in the streamwise direction. The extensional viscosity of HPC is lower compared to PEO, thus HPC is less effective in the streamwise direction.

Since it is considered that the streamwise direction is affected by extensional viscosity, that of polymer solution was measured by an abrupt contraction flow. The force to push water at 5 ml/min was 10 N, which was used to calculate P_F. The density of water was applied to all solution. By using these values, the forces to push the solution at the flow rates of 5, 10, 20 and 30 ml/min corresponding to the extension rate of 13, 26, 52, 78 s^{-1} were 96, 133, 169 and 228 N for PEO solution, 112, 135, 169 and 190 N for HPC solution from the calculation of PEX, respectively. Shear viscosities of the PEO solution was 0.43 Pa s at applied shear stress in glass tube, and that of the HPC solution was 0.59 Pa s. Other scales which need for calculation are shown in Fig. 4a. Calculated extensional viscosities are shown in Fig. 4c. The extensional viscosity of PEO at the applied extension rate is slightly decreased. On the contrary, that of HPC is suddenly decreased at 78 s^{-1}. This result indicates that the extensional viscosity in 2D turbulence at the extension rate of 351 s^{-1} is expected high in the case of PEO, while that of HPC is already low. Thus, the drag reduction in the streamwise direction occurs effectively by PEO, not by HPC. These increase and decrease of the extensional viscosity were due to the extension of PEO and to the orientation of HPC, but the oriented HPC do not make any entangled structures. Thus, the breakup of the structure occurred at relatively low extension rates.

4 Conclusions

An experimental study has been performed in order to investigate how the extensional viscosity of polymers affects on turbulent drag reduction. PEO as a flexible polymer and HPC as a rod-like rigid polymer were added to the 2D turbulence. The power spectra of interference images were obtained, which is related to the water layer fluctuations in turbulence. The scaling behavior of the power spectra gives the information of energy transfer in turbulence. From these results, it was suggested that the mechanism of drag reduction in turbulence is different in normal and streamwise direction. In the normal direction, the orientation of polymers prohibits the energy transfer. On the other hand, the extensional viscosity prohibits the energy transfer in the streamwise direction. The extensional viscosity of polymer solution in an abrupt contraction flow, which indicates the extensional viscosity of HPC was lower than that of PEO at the applied extensional strain in 2D flow. Thus, HPC was less effective in the streamwise direction.

Acknowledgements This study is supported in part by the Grant-in-Aid for Young Scientists(B) (Project No.: 24760129) and the Grant-in-Aid for Scientific Research(B) (Project No.: 24360319) from the Japan Society for the Promotion of Science (JSPS).

References

1. Lumley, J.: Drag reduction in turbulent flow by polymer additives. J. Polym. Sci. **7**, 263–270 (1973)
2. Tabor, M., de Gennes, P.G.: A cascade theory of drag reduction. Europhys. Lett. **2**, 519–522 (1986)
3. Smith, D.E., Chu, S.: Response of flexible polymers to a sudden elongational flow. Science **281**, 1335–1340 (1998)
4. Hidema, R., Furukawa, H.: Development of film interference flow imaging method (FIFI) studying polymer stretching effects on thin liquid layer. e-J. Surf. Sci. Nanotech. **10**, 335–340 (2012)
5. Hidema, R., Ushiki, H., Furukawa, H.: Polymer effects on turbulence in flowing soap films studied with film interference flow imaging method. J. Solid Mech. Mater. Eng. **5**, 838–848 (2011)
6. Kellay, H., Goldburg, W.I.: Two-dimensional turbulence: a review of some recent experiments. Rep. Prog. Phys. **65**, 845–894 (2002)
7. Hidema, R., Yatabe, Z., Shoji, M., Hashimoto, C., Pansu, R., Sagarzasu, G., Ushiki, H.: Image analysis of thickness in flowing soap films. I: Effects of polymer. Exp. Fluids. **49**, 725–732 (2010)
8. McKinley, G.H., Raidford, W.P., Brown, R.A., Armstrong, R.C.: Nonlinear dynamics of viscoelastic flow in axisymmetric abrupt contractions. J. Fluids. Mech. **223**, 411–456 (1991)